Analytica Chimica Acta 798 (2013) 33–39

Contents lists available at ScienceDirect

Analytica Chimica Acta

journal homepage: www.elsevier.com/locate/aca

An aptasensor for sensitive detection of human breast cancer cells by using porous GO/Au composites and porous PtFe alloy as effective sensing platform and signal amplification labels

Mei Yan[a], Guoqiang Sun[a], Fang Liu[a], Juanjuan Lu[a], Jinghua Yu[a,*], Xianrang Song[b,*]

[a] Key Laboratory of Chemical Sensing & Analysis in Universities of Shandong, School of Chemistry and Chemical Engineering, University of Jinan, Jinan 250022, PR China
[b] Cancer Research Center, Shandong Tumor Hospital, Jinan 250012, PR China

HIGHLIGHTS

- Aptamer biosensor for MCF-7 cells based on ultrasensitive electrochemical detection.
- Porous GO/Au composites and porous PtFe alloy were used as effective sensing platform and signal amplification labels.
- PEG not only as an excellent reductant, it can also make Au nanoparticles uniformly distributed in the GO/Au composites.

GRAPHICAL ABSTRACT

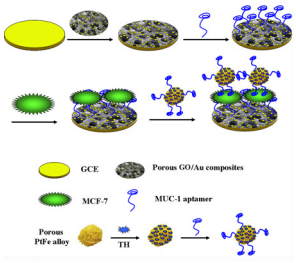

ARTICLE INFO

Article history:
Received 3 July 2013
Received in revised form 21 August 2013
Accepted 27 August 2013
Available online 31 August 2013

Keywords:
Nanoporous materials
Porous PtFe alloy
Aptamer
MCF-7
Biosensor

ABSTRACT

A novel aptamer biosensor for cancer cell assay has been reported on the basis of ultrasensitive electrochemical detection. The assay uses the aptamer as a capture probe to recognize and bind the tumor marker on the surface of the cancer cells, forming an aptamer-based sandwich structure for MCF-7 cells detection. Functionalized nanoporous materials, porous graphene oxide/Au composites (GO/Au composites) and porous PtFe alloy have been introduced into the biosensor. Owing to the large surface area and versatile porous structure, the use of nanoporous materials can significantly improve the analysis performance of the biosensors by loading of large amounts of molecules and accelerating diffusion rate. Under the optimized experimental conditions, the proposed aptamer biosensor exhibited excellent analytical performance for MCF-7 cells determination, ranging from 100 to 5.0×10^7 cells mL^{-1} with the detection limit of 38 cells mL^{-1}. The biosensor showed good selectivity, acceptable stability and reproducibility, and developed a highly sensitive and selective method for cancer cells detection.

1. Introduction

Cancer is a main cause of the worldwide death and there is an estimated 17 million deaths in 2030 which is learnt from World Health Organization. Among them, breast cancer is the second common type of cancer after lung cancer and the fifth common cause of cancer death [1]. Although significant progress has been made in both the understanding and treatment of this cancer during the last few decades, it still remains one of the leading causes of death [2]. The distant metastases are regarded as the major reason to cause cancer death. Thus, early diagnosis and timely therapy have been considered to be the most effective ways to improve survival rate at present [3]. Despite the diagnostic improvements [4,5], highly sensitive and selective detection of cancer cells is still a challenge for the diagnosis and treatment

* Corresponding authors. Tel.: +86 531 82767161.
E-mail addresses: ujn.yujh@gmail.com, 306375767@qq.com (J. Yu), sxr@vip.163.com (X. Song).

0003-2670/$ – see front matter © 2013 Elsevier B.V. All rights reserved.
http://dx.doi.org/10.1016/j.aca.2013.08.046

of cancer [6,7]. Therefore, the development of new techniques to unambiguously, simply and rapidly identify and characterize the tumor cells has been of great importance [8,9].

The general techniques for detection of cancer cells include immunophenotyping by flow cytometry [10] or microarray [11] and amplification of malignant cell mutations by PCR [12]. However, these methods suffering from false-positivity/negative results, time consuming and lack of efficiency [13,14]. In recent years, the aptamer-based bioassay has attracted tremendous interests because of its excellent properties. Aptamers, which are singe strand nucleic acid capable of binding to their target molecules with high affinity and specificity, are selected by SELEX (systematic evolution of ligands by exponential enrichment). Aptamers have many advantages over traditional recognition molecules such as ease of synthesis and modification, good stability during long-term storage, nontoxicity, and lack of immunogenicity. For cellular study, aptamers have been used to distinguish different cell lines and identify the native protein targets on the cell surface [15–17]. In this work, we select the mucin 1 proteins (MUC-1) as a tumor maker in human breast carcinoma MCF-7 cells. The MUC-1 is a cell-surface associated glycoprotein, which is highly expressed by the majority of adenocarcinomas and, in particular, by the primary and metastatic breast cancers [18,19]. Some others have developed a few methods to detect MUC1-overexpressed breast cancer cells [20–24]. In this paper, aptamer-based electrochemical method was used for MCF-7 cells sensing, it not only have the advantages of electrochemical sensors, such as rapid response, high sensitivity, ease of use, low cost and small-sized commercial detectors, but also inherit the high affinity and specificity of aptamers.

To further improve the sensitivity for cell detection, nanomaterials with unique physical and chemical properties and the unusual biomolecule binding capabilities [25,26] have contributed a lot in increasing the sensing surface area and amplifying the signal output. Recently, nanoporous materials have found increasing applications in many areas, including bioengineering [27], catalysis [28], and biosensing [29], due to their large surface area, tailored pore size distribution, controllable pore structure, and versatile composition. Especially for biosensors, the use of nanoporous materials can significantly improve the analysis performance of the biosensors since their large surface area and versatile porous structure are beneficial for the loading of large amounts of molecules and accelerating diffusion rate.

In this work, a novel porous graphene oxide/Au composites (GO/Au composites) with large specific surface area and good electrical conductivity were synthesized to modify working electrode for cells recognition. Compared with the conventional 2D crystal lattice graphene, the porous graphene dramatically improved the specific surface area, electrical conductivity and mechanical stiffness [30]. Combined with Au nanoparticles, porous GO/Au composites possess fast electron transportation good biocompatibility. Furthermore, thionine (TH) functionalized nanoporous PtFe alloy as signal amplification for cells detection. Xu's group reported the porous PtFe alloy nanostructure exhibits superior electrocatalytic activity for methanol oxidation reaction [32]. However, there was no related research of porous PtFe alloy in biosensing. Hereon, porous PtFe alloy were used as signal molecule and aptamer immobilization carriers due to their highly accessible surface areas and rich surface chemistry.

Based on the advantages mentioned above, an ultrasensitive biosensor was designed using porous GO/Au composites modified electrode, which constructed an effective biomolecules immobilization matrix and made the immobilized biomoleculers possessed high stability and bioactivity. In addition, the amplified sensitivity was enhanced by using signal molecule TH modified porous PtFe alloy as labels. The experimental results showed that the aptamer biosensor exhibited excellent analytical performance for MCF-7 detection.

2. Experimental

2.1. Chemicals

Chemicals and materials: graphite powder (KS-10, 99.95%), 6-mercapto-1-hexanol (MCH) was obtained from Sigma–Aldrich. Polyethylene glycol (PEG) was purchased from Nektar (Huntsville, AL). Bovine serum albumin (BSA, 96–99%), Gold chloride ($HAuCl_4{\cdot}4H_2O$) and TH were purchased from Sigma Chemical Co. (St. Louis, MO, USA). Phosphate buffered solutions (PBS) were prepared using 0.01 mol L^{-1} KH_2PO_4 and 0.01 mol L^{-1} Na_2HPO_4. All other reagents were of analytical reagent grade and used without further purification. Ultrapure water obtained from a Millipore water purification system (≥18 MΩ, Milli-Q, Millipore) was used in all assays and solutions.

The human breast cancer cells MCF-7 cell lines were used as target cells, HepG2 cells and SK-BR-3 cells were used as control cells. They were provided by Shandong Tumor Hospital. MCF-7 cells were cultured in RPMI 1640 medium containing 10% fetal calf serum, 100 U mL^{-1} penicillin, and 100 μg mL^{-1} streptomycin in 5% CO_2 at 37 °C.

All oligonucleotides used in this study were purchased from Sangon Biotech Co., Ltd. (Shanghai, China), and the sequences of oligonucleotides were as follows:

MUC-1 aptamer(S1): 5′-GCA GTT GAT CCT TTG GAT ACC CTG G-NH_2-3′.

2.2. Apparatus

The ECL experiments were carried out on a MPI-B multiple-parameter chemiluminescence analytical testing system equipped with a MPI-A B^{-1} multifunction chemiluminescence detector (Xi'An Remax Electronic Science & Technology Co., Ltd. Xi'an, Changchun Institute of Applied Chemistry Chinese Academy Sciences, China) at room temperature. Electrochemical measurements were carried out with a CHI 660D electrochemistry workstation (Shanghai CH Instruments Co., China) Electrochemical impedance spectroscopy (EIS) was performed on a CHI 604D Electrochemical Workstation (Shanghai CH Instruments Inc., China). All experiments were carried out with a conventional three-electrode system with glassy carbon electrode (GCE) as the working electrode (WE), a platinum counter electrode (CE) and an Ag/AgCl (sat. KCl) reference electrode (RE). Scanning electron microscopy (SEM) images were recorded using a JEOL-JSM-6300 scanning electron microscope. Transmission electron microscopy (TEM) images were obtained from a Hitachi H-800 microscope (Japan). High resolution transmission electron microscopy (HRTEM) image of the prepared C-dots was recorded on an electronic microscopy (Tecnai G2 F20S5TWIN 200 KV). Atomic force microscope (AFM) images were achieved by scanning probe microscopy (SPM, Vecco, USA).

2.3. Synthesis of porous GO/Au composites

The porous GO/Au composites were prepared by hydrothermal method using GO as precursor. The GO was synthesized from natural graphite powder by an improved Hummers method [31]. GO was dissolved in water with the concentration of 5 mg mL^{-1}. The suspension was disrupted into a homogeneous solution using an ultrasonic cell crusher for 60 min. Then, the homogeneous GO solution was prepared. In order to obtain a better porous GO/Au composites, we used sodium citrate and PEG as reducing agent respectively. The detailed preparation steps are as follows: GO (10 mL, 0.5 mg mL^{-1}), $HAuCl_4{\cdot}4H_2O$ (200 μL, 1%, w w^{-1}) and 20 μL

PEG (sodium citrate, 1%) were mixed uniformity in an ultrasonic bath for 1 h, and then reacted in 180 °C for 12 h. After cooling to room temperature, the mixture was washed three times with water. Finally, the porous GO/Au composites were obtained through freeze drying process. The formation of a columnar ice phase and subsequent drying produced graphene structures of a few microns in diameter. The resulting porous GO/Au composites were redispersed in PBS.

2.4. Synthesis of nanoporous PtFe alloy

The nanoporous PtFe alloy was straightforwardly fabricated by means of mild de-alloying of the PtFeAl source alloy according to Xu et al.'s reported method [32]. Briefly, $Pt_{11}Fe_9Al_{80}$ (atomic %) ternary alloy foils were prepared by refining pure (>99.9%) Pt, Fe, and Al in an arc furnace, followed by melt-spinning under an argon-protected atmosphere. Nanoporous PtFe alloy were prepared by selectively etching the $Pt_{11}Fe_9Al_{80}$ in 2.0 mol mL^{-1} NaOH solution for 48 h at room temperature. During the preparation of carbon-supported PtFe/C nanoparticles, Vulcan XC-72 carbon black was pretreated in 6 mol mL^{-1} HNO_3 solution at 100 °C for 4 h [33] and a feeding mole ratio between platinum and iron is controlled at 55:45. The other procedure was operated completely according to the work by Xu et al. [34].

2.5. Preparation of reporter probe S1/TH/PtFe bioconjugates

The prepared nanoporous PtFe alloy was redispersed into 2 mL of TH aqueous solution (2 mmol L^{-1}) and slightly stirred at 150 rpm for 1 h at room temperature to get TH/PtFe composites. The reaction is based on the interaction between $-NH_2$ groups on TH and Pt [35]. After centrifugation and washing, the TH/PtFe composites were redispersed into glutaraldehyde solution (100 μL, 2.5%, w w^{-1}), followed by adding S1 solution (1 mL, 50 μM). After incubating for 2 h at 4 °C with gentle stirring, the mixture was washed with buffer solution, and centrifuged (7000 rpm, 3 min) for three times. Following that, the precipitation was added into 1.0 wt% BSA solution to block possible remaining active sites and diluted to 0.5 mL with PBS. The as-prepared S1/TH/PtFe bioconjugates were stored at 4 °C unless use. The preparation process was shown in Fig. 1. The electroactive label molecule (TH) was assembled on the nanoporous PtFe alloy. Under the electrochemical assays, the electrochemical signal of TH was measured, which was proportional to the amount of the concentration of MCF-7 cells.

2.6. Preparation of S1/GO/Au modified electrode

The GCE with a diameter of 3 mm was firstly polished using 1.0, 0.3 and 0.05 μm alumina slurry prior to use, followed by successive sonication in ethanol and dried in air at room temperature. Then, 5 μL porous GO/Au composites were deposited on the electrode surface, and then dried at room temperature. After that the modified electrode was immersed into 10 mM Tris–HCl (pH 7.4) containing 1 μM S1, 0.1 mM EDTA, 0.1 M NaCl and 10 mM TCEP for 2 h. S1 could be assembled on the surface of GO/Au composites modified electrode effectively. The reaction is based on the interaction between NH_2 groups on S1 and Au. Followed by 1 h treatment with 2 mM MCH and thoroughly rinsed with doubly distilled water, the S1/GO/Au modified electrode was thus prepared and ready for the following experiments.

2.7. Assembly of cells onto modified electrode and electrochemical detection

After washing with water, 10 μL of PBS containing different number of MCF-7 cells were dropped on the modified electrode

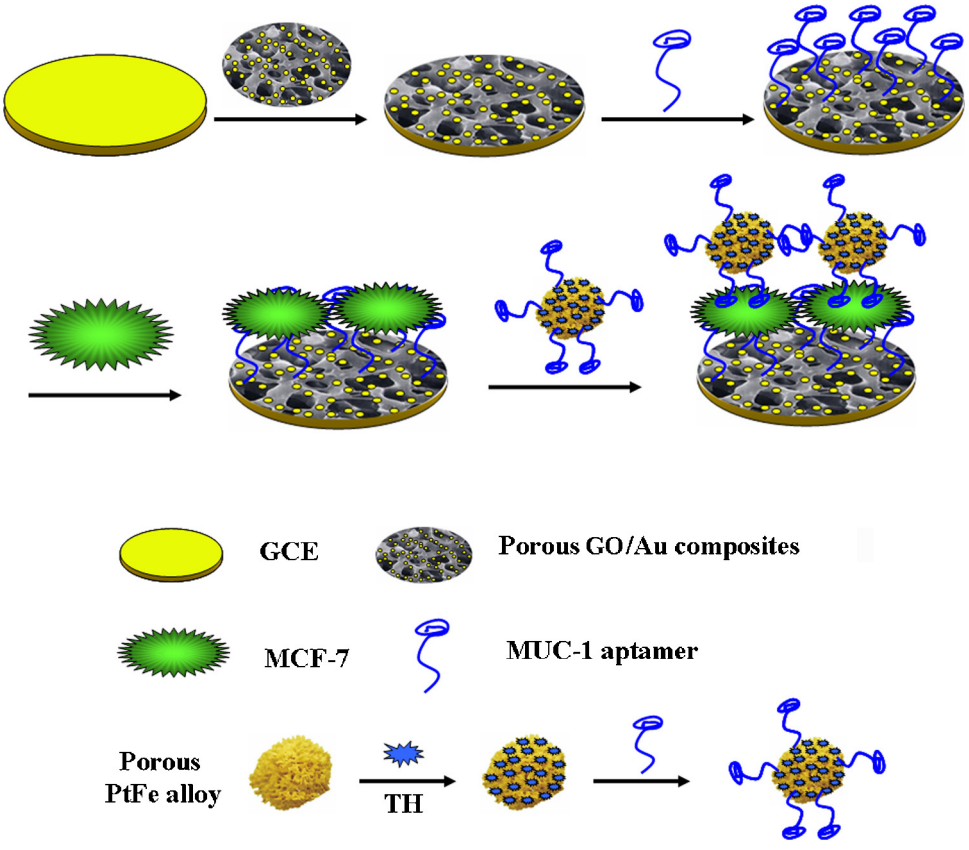

Fig. 1. Schematic representation of fabrication process of S1/TH/PtFe composites and the aptamer biosensor for MCF-7 cells.

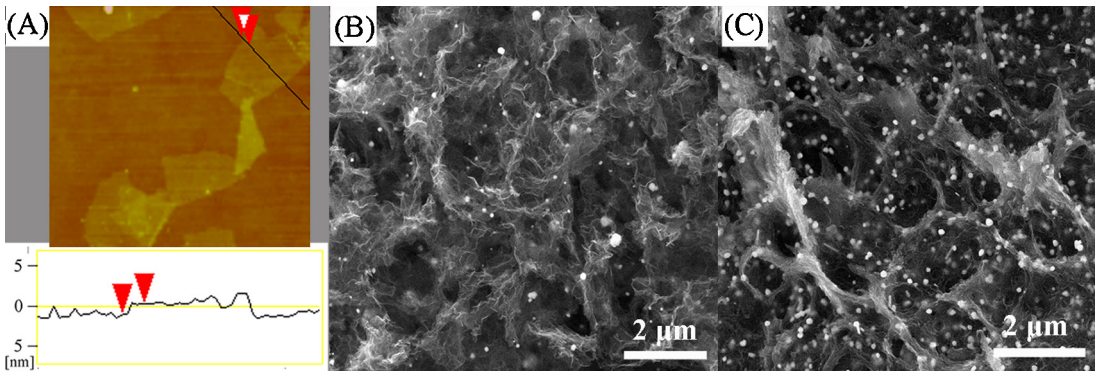

Fig. 2. AFM image of GO (A), SEM image of porous GO/Au composites using sodium citrate (B) and PEG (C) as reducing agent respectively.

to hybridize with S1 aptamers at 37 °C for 2 h, and then washed with PBS. After that the S1/GO/Au modified electrode which was assembled with MCF-7 cells was firstly immersed in a 100 μL PBS containing 0.5% Tween-20 and 1% BSA at the room temperature for 30 min. Then it was rinsed twice with pH 7.4 PBS. Eventually, the electrode was incubated with the S1/TH/PtFe bioconjugates solution for 2 h. Followed by washing with PBS to remove the excrescent matter, the constructed biosensor was ready for electrochemical measurement. The fabrication procedure was represented in Fig. 1. The analytical principle of this electrochemical biosensor was based on dual-recognition of MUC-1 aptamer (modified on the electrode and nanoporous PtFe alloy) and MCF-7 cells, which is forming an aptamer-cell-aptamer sandwich architecture. Under the electrochemical assays, the electrochemical signal of TH (assembled on the nanoporous PtFe alloy) was measured, which was proportional to the amount of TH molecules and further corresponded to the amount of the concentration of MCF-7 cells.

EIS, cyclic voltammetry (CV) and differential pulse voltammetry (DPV) were employed to study the electrochemical behavior of the biosensor and to characterize the detection efficiency.

3. Results and discussion

3.1. Characterization of porous GO/Au composites

The porous GO/Au composites were prepared by hydrothermal method using GO as precursor. Fig. 2(A) is the typical AFM images and height profiles of GO. The thickness of the GO sheet obtained is about 1 nm, which is consistent with previously reported thickness of GO sheets [36]. Fig. 2(B) and (C) was SEM images of the prepared porous GO/Au composites using sodium citrate and PEG as reducing agent, respectively. From the images we can see that the surface structure of porous GO/Au composites. It was clear to see that a better porous structure and dispersity of Au nanoparticles were obtained in Fig. 2(C). It was indicated that PEG not only as an excellent reductant, it can also make Au nanoparticles uniformly distributed in the composites. As shown in Fig. 2(C), Au nanoparticles distributed not only on the surface but also in the internal of GO uniformly. As the porous structures gave a high specific surface area, it was able to provide a large surface area for aptamer attachment. More importantly, the internal doped AuNPs were expected to enhance electronic transmission rate.

3.2. Characterization of nanoporous PtFe alloy

Fig. 3(A) and (B) shows the SEM and TEM images of nanoporous PtFe alloy, respectively. As shown in Fig. 3(A), the nanoporous PtFe alloy displays a type of 3D spongy-like morphology. The porous structure was resulted from de-alloying of the PtFeAl alloy. Nanoporous PtFe alloy with nanoporous structure and good biocompatibility was expected to enhance the immobilized amount of signal molecule (TH) and aptamer (S1) due to its large surface area and versatile porous structure nanoporous. In addition, the high conductivity and porosity can improve the electron transfer rate of the biosensor.

3.3. Characterization of electrochemical measurements

The electrochemical detection was performed by using a sandwich model for the capture of MCF-7 cells. The electroactive label molecules (TH) and capture aptamer (S1) were assembled on the surface of nanoporous PtFe alloy. The aim of using nanoporous PtFe alloy is to amplify the voltammetric signals and to enhance the detection sensitivity. When the prepared electrochemical biosensor was ready for electrochemical assay, the signal was measured, which was proportional to the amount of the signal molecules and further corresponded to the concentration of MCF-7 cells.

EIS is an effective method to monitor the changes of interfacial properties, allowing the understanding of chemical transformation and processes associated with the conductive electrode surface [37]. We use this method to get information on the impedance changes of the biosensor interface in the assembling process. Electrochemical impedances of the MCF-7 biosensor were performed with addition of a background solution of 5.0 mmol L^{-1} $Fe(CN)_6^{4-/3-}$ containing 0.1 mmol L^{-1} KCl, and the frequency range is at 100 mHz to 10 kHz at 220 mV. Fig. 4(A) showed a Nyquist plot of impedance for the stepwise modification process on the GCE. The curve (a) showed the EIS of bare GCE after polishing, there is a small semicircle (Ret = 163 Ω) at high frequencies and a linear part at low frequencies. However, when porous GO/Au composites were modified on the GCE surface, the EIS of GO/Au/GCE displayed an almost straight line in the Nyquist plot (curve b), indicating that the introduction of the AuNPs was highly beneficial to the electron transfer. When capture aptamer (S1) was immobilized on the surface of GO/Au/GCE, the Ret increased to 290 Ω (curve c), which was due to the immobilization of negatively charged probes ssDNA sequence on the electrode surface that could result in a negatively charged interface and repelled the negatively charged redox probe $[Fe(CN)_6]^{3-/4-}$ electrostatically. Moreover, further increase of the resistance can be observed when target cells are introduced in sequence (curve d, Ret = 1028 Ω), which were caused by the nonconductive properties of biomacromolecule. At last, When reporter probe S1/TH/PtFe bioconjugates were recognition with MCF-7 cells (curve e), interestingly the resistance decreased to 820 Ω, indicating that the synthesized S1/TH/PtFe bioconjugates possessed high conductivity and good electron transfer efficiency, although the aptamer layer acted as barrier to the interfacial electron transfer.

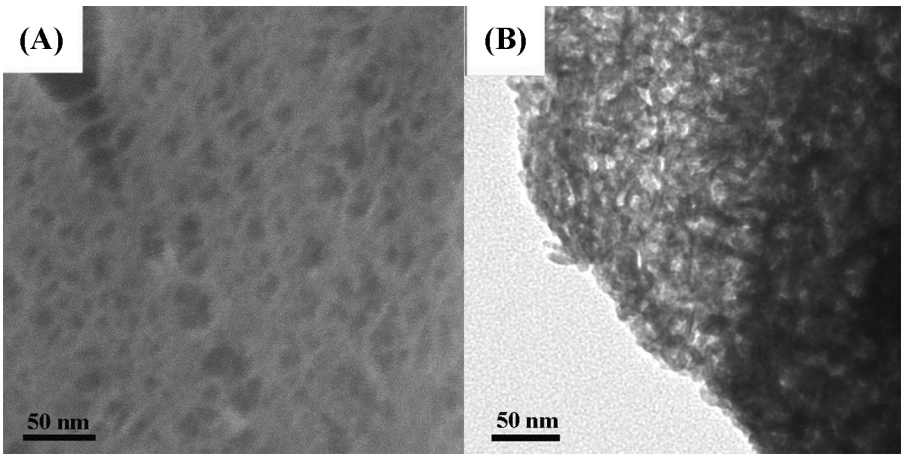

Fig. 3. SEM (A) and TEM (B) image of porous PtFe alloy.

3.4. Comparison of electrochemical responses

In this contribution, the assay is based on a sandwich-type format using porous GO/Au composites modified electrode as capture substrate and S1/TH/PtFe bioconjugates as traces. So, the performance of modified electrode and signal labels are crucial. In order to verify the performance of porous GO/Au composites modified electrode, a comparative study of the electrochemical responses of the biosensor was carried out on different modified electrode. The results were shown in Fig. 4(B). Compared with bare GCE (curve a), the current response increased when graphene modified on GCE surface (curve b), implying that the graphene is an excellent electric conducting material which can accelerate the electron transfer. However, when porous GO/Au composites modified on GCE, the current response increased significantly (curve c), indicating that the porous GO/Au composites possessed high conductivity and good electron transfer efficiency. In contrast, for GO modified GCE, cathodic and anodic peak currents decreased obviously (curve d), the reason is that GO has low conductivity. The advantages of as-prepared porous GO/Au composites modified electrode are considered as follows: (i) the porous GO could display a high surface-to-volume ratio, which could enhance the immobilized amount of biomolecules; (ii) Au nanoparticles with high conductivity and good biocompatibility were penetrated/coated into/onto porous GO materials, which could further amplify the specific surface area and enhance the sensitivity of the biosensor. Meanwhile, owing to the porous structure and high specific surface area, the nanoporous PtFe alloy can load a large amount of electroactive label molecules (TH) and capture aptamer (S1), which can significantly improve the sensitivity of MCF-7 cells detection. Hence, the proposed biosensor and assays could display better analytical properties under the same conditions.

3.5. Optimization of experimental variables

The incubation time was an important parameter for both capturing MCF-7 on the electrode surface and specifically recognizing S1/TH/PtFe bioconjugates. Different incubation time was tested ranging from 1 h to 4 h. The experimental results show that the electrochemical response increases with increasing incubation time of MCF-7 cells and tends to a steady value after 2 h, indicating a thorough capturing of MCF-7 cells on the electrode surface. In the second recognization step, the current shows the same changing tendency, and the response current reached a plateau at about 2 h. Therefore, the optimal incubation time is 2 h.

The pH value of the measuring solution is an important parameter for the aptamer sensor response signals. Unsuitable pH can damage the structure and performance of DNA, which could reduce the efficiency of recognization and affect the affinity between DNA and the electrode surface. Hence, a series of PBS with the pH values from 6.0 to 8.5 were tested. The results indicated that the aptamer sensor displayed an optimum sensitivity of the response at pH 7.4, and the current response decreased if the pH higher or lower than this value.

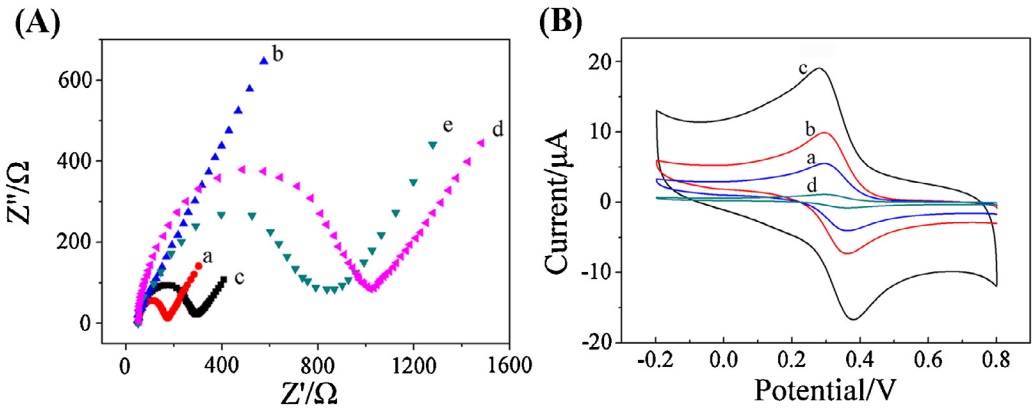

Fig. 4. (A) EIS of different modified electrode: (a) bare GCE, (b) GO/Au/GCE, (c) S1/graphene/Au/GCE, (d) MCF-7/S1/graphene/Au/GCE, (e) S1/TH/PtFe bioconjugates MCF-7/S1/GO/Au/GCE in 5.0 mmol L^{-1} $Fe(CN)_6^{4-/3-}$ containing 0.1 mmol L^{-1} KCl, and the frequency range is at 100 mHz to 10 kHz at 220 mV. (B) Cyclic voltammograms of bare GCE (a), graphene/GCE (b), GO/Au/GCE (c) and GO/GCE (d) in 2 mmol L^{-1} potassium ferricyanide solution (pH 7.0) containing 0.1 mol L^{-1} KCl at 50 mV s^{-1}.

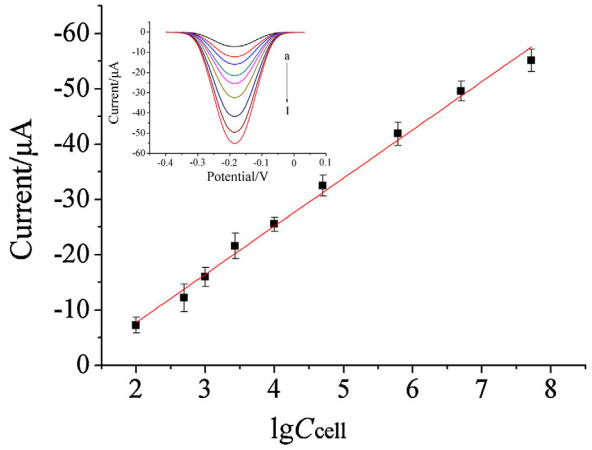

Fig. 5. Calibration curves of the electrochemical biosensor toward target cells concentration in supporting electrolyte (inset picture is the corresponding response curves). 10 mmol L^{-1} PBS solution (pH 7.4) as supporting electrolyte. The concentration of cells were as follows: 1.0×10^2, 5.0×10^2, 1.0×10^3, 3×10^3, 1.0×10^4, 5.0×10^4, 5.0×10^5, 5.0×10^6, 5.0×10^7 cells mL^{-1}.

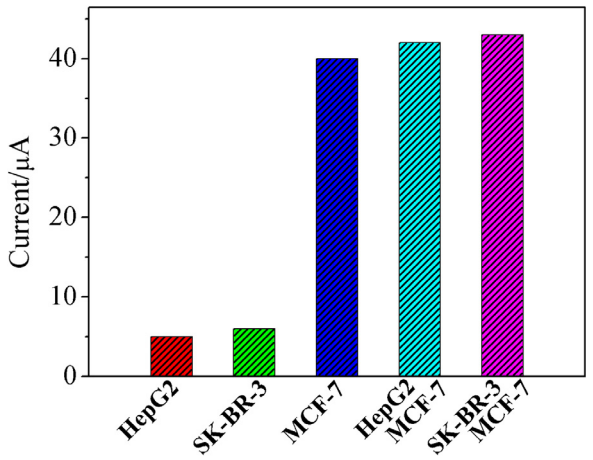

Fig. 6. DPV responses for different cells. The concentrations were 5.0×10^5 cells mL^{-1} respectively.

3.6. The analytical performance of ECL aptamer sensor

Under the optimized experimental conditions, we investigated the performance of the developed electrochemical aptamer biosensor in quantitative analysis of cancer cells. The peak currents of the biosensor were linearly proportional to the logarithm of target MCF-7 cells concentration. The sensitivity of the developed biosensor was investigated by varying the concentration of MCF-7 cells with the sensitive different pulse voltammetric detection. As shown in Fig. 5, the reduction peak current increased gradually with the increase in the MCF-7 cell concentration. The average reduction peak current had a good linear relationship versus the logarithm of concentration of MCF-7 cell in the range from 100 to 5.0×10^7 cells mL^{-1} with a correlation coefficient of 0.994. The linear regression equation was calculated as $I = 9.71 - 8.72\lg (C_{MCF\text{-}7}$, cells $mL^{-1})$ with a detection limit (LOD) of 38 cell mL^{-1} at a signal-to-noise ratio of 3σ (where σ is the standard deviation of the blank solution, $n = 11$), which was comparable to those reported by most of aptamer-based assays [38] and other electrochemical and fluorescence cytosensing strategy for cancer cell detection [39,40].

3.7. Selectivity, reproducibility, stability of the cell-based biosensor

In order to evaluate the selectivity, the platform was performed using MCF-7 cells, HepG2 cells and SK-BR-3 cells and artificial complex samples by mixing equal amounts of MCF-7 cells and HepG2 cells, MCF-7 cells and SK-BR-3 cells, respectively. As illustrated in Fig. 6, HepG2 cells, SK-BR-3 cells showed a little response for they are MUC1-negative cells. However, a well-defined current increasing was obtained for MCF-7 cells and artificial complex samples. The comparative results show that the proposed aptamer biosensor has an excellent selectivity to MCF-7 cells.

The reproducibility of the aptamer sensor was examined. Sensing interfaces prepared on the same and on different electrodes were used to detect MCF-7 cells with the same concentration. Standard deviation of five dependent measurements was less than 5% for the same electrode, and less than 8% for different electrodes. Thus, the aptamer biosensor has a relatively good reproduction in detection.

Stability of this aptamer sensor is a key factor in their application and development. When the aptamer biosensor was dried and stored at 4 °C, it retained at 90% of its initial response after a storage period of 30 days, indicating the proposed cell-based biosensor had stable storage stability.

4. Conclusions

In summary, a novel electrochemical aptamer biosensor was developed for cancer cell detection based on aptamer-aided cell recognition. The use of aptamers provide this technique with good specificity for identification of cancer cells, and porous GO/Au composites modified electrode as capture substrate and S1/TH/PtFe bioconjugates as traces allows highly efficient amplification of cell capturing events. Using MCF-7 cells as model case, the developed strategy was demonstrated to display high selectivity in discriminating MCF-7 cells, detection limit as 38 cells mL^{-1}, and a wide linear response range from 100 to 5.0×10^7 cells mL^{-1} with desirable reproducibility. Since this method can be more kinds of tumor cells by altering the related aptamers for different kinds of tumor markers in accordance with the clinic demands, thus it provides a significant tool for detecting the cancer cells in the process of disease progression and understanding biological processes related to cancers.

Acknowledgements

This work was financially supported by Natural Science Research Foundation of China (21277058, 21175058, 51003039, 51273084), Natural Science Foundation of Shandong Province, China (ZR2012BZ002, ZR2011BQ019).

References

[1] P. Boyle, B. Levin, World Cancer Report, International Agency for Research on Cancer, France, 2008.
[2] M. Lacroix, Endocr. Relat. Cancer 13 (2006) 1033–1067.
[3] X. Yucai, T. Yin, W. Wiegraebe, X.C. He, D. Miller, D. Stark, K. Perko, R. Alexander, J. Schwartz, J.C. Grindley, J. Park, J.S. Haug, J.P. Wunderlich, H. Li, S. Zhang, T. Johnson, R.A. Feldman, L. Li, Nature 457 (2009) 97–101.
[4] R. Weissleder, M.J. Pittet, Nature 452 (2008) 580–589.
[5] E.I. Sega, P.S. Low, Cancer Metast. Rev. 27 (2008) 655–664.
[6] H.Z. Chen, S.Y. Tsai, G. Leone, Nat. Rev. Cancer 9 (2009) 785–797.
[7] B. Sarkar, J. Dosch, D.M. Simeone, Chem. Rev. 109 (2009) 3200–3208.
[8] J.C. Ehrhart, B. Bennetau, L. Renaud, J.P. Madrange, L. Thomas, J. Morisot, A. Brosseau, S. Allano, P. Tauc, P.L. Tran, Biosens. Bioelectron. 24 (2008) 467–474.
[9] L. Liu, X. Zhu, D. Zhang, J. Huang, G. Li, Electrochem. Commun. 9 (2007) 2547–2550.
[10] R.P. Aguilera, L.R. Guzman, N.L. Santiago, L.B. Ceron, O.C. Monte, S.N. Martinez, Am. J. Hematol. 68 (2001) 69–74.
[11] L. Belov, O. Vega, C.G. Remedios, S.P. Mulligan, R.I. Christopherson, Cancer Res. 61 (2001) 4483–4489.
[12] R.A. Ghossein, S. Bhattacharya, J. Cancer 36 (2000) 1681–1694.

[13] C. Pan, M. Guo, Z. Nie, X. Xiao, S. Yao, Electroanalysis 21 (2009) 1321–1326.
[14] E.M. Eltahir, D.S. Mallinson, G.G. Birnie, C. Hagan, W.D. George, A.D. Purushotham, Br. J. Cancer 77 (1998) 1203–1207.
[15] C.F. Ding, Y. Ge, S.S. Zhang, Chem. Eur. J. 16 (2010) 10707–10714.
[16] W. Li, X.H. Yang, K.M. Wang, W.H. Ta, Y. He, Q.P. Guo, H.X. Tan, J.B. Liu, Anal. Chem. 80 (2008) 5002–5008.
[17] G.X. Li, P. Miao, Electrochemical Analysis of Proteins and Cells, Springer, Berlin, Germany, 2012.
[18] C.S.M. Ferreira, C.S. Matthews, S. Missailidis, Tumor Biol. 27 (2006) 289–301.
[19] C.D. Pieve, A.C. Perkins, S. Missailidis, Nucl. Med. Biol. 36 (2009) 703–710.
[20] T. Li, Q. Fan, T. Liu, X. Zhu, J. Zhao, G. Li, Biosens. Bioelectron. 25 (2010) 2686–2689.
[21] J. Zhao, X. He, B. Bo, X. Liu, Y. Yin, G. Li, Biosens. Bioelectron. 34 (2012) 249–252.
[22] W. Wei, D. Li, X. Pan, S. Liu, Analyst 137 (2012) 2101–2106.
[23] J. Li, X. Zhong, F. Cheng, J. Zhang, L. Jiang, J. Zhu, Anal. Chem. 84 (2012) 4140–4146.
[24] X. Zhu, J. Yang, M. Liu, Y. Wu, Z. Shen, G. Li, Anal. Chim. Acta 764 (2013) 59–63.
[25] N.J. Ronkainen, H.B. Halsall, W.R. Heineman, Chem. Soc. Rev. 39 (2010) 1747–1763.
[26] M.M. Rahman, A.J.S. Ahammad, J.H. Jin, S.J. Ahn, J.J. Lee, Sensor 10 (2010) 4855–4886.
[27] X.Y. Yang, Z.Q. Li, B. Liu, Adv. Mater. 18 (2006) 410–414.
[28] Y. Wan, H.Y. Wang, Q.F. Zhao, J. Am. Chem. Soc. 131 (2009) 4541–4545.
[29] S. Wu, H.X. Ju, Y. Liu, Adv. Funct. Mater. 17 (2007) 585–592.
[30] Y.C. Yong, X.C. Dong, M.B.C. Park, H. Song, P. Chen, ACS Nano 6 (2012) 2394–2400.
[31] D.C. Marcano, D.V. Kosynkin, J.M. Berlin, A. Sinitskii, Z.Z. Sun, A. Slesarev, ACS Nano 4 (2010) 4806–4814.
[32] C.X. Xu, Q. Li, Y.Q. Liu, J.P. Wang, H.R. Geng, Langmuir 28 (2012) 1886–1892.
[33] H. Zhao, L. Li, J. Yang, Y. Zhang, H. Li, Electrochem. Commun. 10 (2008) 876–879.
[34] J. Xu, K. Hua, G. Sun, C. Wang, X. Lv, Y. Wan, Electrochem. Commun. 8 (2006) 982–986.
[35] S. Mandal, D. Roy, R.V. Chaudhari, M. Sastry, Chem. Mater. 16 (2004) 3714–3724.
[36] D.C. Marcano, D.V. Kosynkin, J.M. Berlin, A. Sinitskii, Z.Z. Sun, A. Slesarev, L.B. Alemany, W. Lu, J.M. Tour, ACS Nano 4 (2010) 4806–4814.
[37] M. Prodromidis, Electrochim. Acta 55 (2010) 4227–4233.
[38] C.F. Pan, M. Guo, Z. Nie, X.L. Xiao, S.Z. Yao, Electroanalysis 21 (2009) 1321–1326.
[39] M. Xie, J. Hu, Y.M. Long, Z.L. Zhang, H.Y. Xie, D.W. Pang, Biosens. Bioelectron. 24 (2009) 1311–1317.
[40] X.R. Zhang, S.G. Li, X. Jin, X.M. Li, Biosens. Bioelectron. 26 (2011) 3674–3678.